RELATIVE PERFORMANCE OF HATCH AND THREE OTHER TECHNIQUES FOR ATMOSPHERIC CORRECTION OF HYPERION AND AVIRIS DATA

Alexander F. H. Goetz,[1,2] Bruce Kindel,[1] Mario Ferri,[3] and Ethan Gutmann[1,2]

1.0 Introduction

The analysis of hyperspectral image data requires either the application of a radiative transfer model to correct radiance data from the sensor to reflectance or the simultaneous acquisition of surface spectral reflectance data to obtain correction factors for the solar irradiance and atmospheric transmission and scattering. The transmission, and in some cases the scattering, is highly location dependent because the major absorber is water vapor, a poorly mixed gas. Therefore, radiative transfer modeling is required to extend point measurements to the rest of the image.

Several models have been developed for atmospheric correction and four of them, ATREM (Gao et al., 1993), HATCH (Qu et al., 2003), ACORN (Miller, 2002) and FLAASH (Matthew et al., 2000) have gained prominence. The latter two are commercially available. In this paper we describe the results of using model and measured reflectances propagated to the top of the atmosphere using MODTRAN4 (Adler-Golden et al., 1999) and retrieved using the above models for different precipitable water vapor values. In addition, we have applied the models to AVIRIS and Hyperion data in order to compare the average reflectances obtained with each model, and compared the results for the derivation of spectral reflectance under a variety of precipitable water vapor conditions.

2.0 Approach

The methods used here are an extension of those described by Goetz et al. (2003). In order to eliminate the variables of sensor response and signal-noise ratio, and the uncertainties in ground reflectance in the comparison of models, the above-the-atmosphere radiance for several total precipitable water vapor values was modeled using MODTRAN4 (Adler-Golden et al., 1999). The modeled at-sensor radiance was entered into the four atmospheric correction models and the surface reflectance retrieved. MODTRAN4 was used to retrieve the modeled radiance to assure the validity of the at-sensor radiance values. A spectrum consisting of 50% reflectance values over the wavelength range 0.4-2.5 μm was input to MODTRAN4 for precipitable water vapor values of 0.5, 1.5, 2.5 and 4.5 cm. This artificial reflectance spectrum was created to emphasize the model differences since there were no slopes or absorption features normally associated with natural materials.

There are errors induced into the retrieval if the wavelength calibration of the sensor departs from that of the model. Reduction of at-sensor radiance to reflectance requires taking a ratio between the modeled and actual radiance that will accentuate wavelength calibration errors especially at the edges of atmospheric absorption bands (Qu et al., 2003). The differences between models as well as the calibration errors are the major contributors to the uncertainty in the retrieval of surface reflectance. The comparison of the ratio between two MODTRAN4 models, incorporating a wavelength shift in one of them, and the retrievals of the 50% spectrum discussed above make it possible to quantify the errors and their sources.

The individual models were applied to field spectra representing pure soil and pure vegetation cover at the four different precipitable water vapor amounts in order to examine the model behavior. This test was important because each model uses a different interpolation scheme and the results differ.

The models were also applied to AVIRIS and Hyperion images having varying average water vapor values. Water vapor images were created and compared. A mean reflectance spectrum was calculated for each entire image so that any sensor influences, such the signal-to-noise ratio, were minimized.

[1] Center for the Study of Earth from Space
[2] Department of Geological Sciences, University of Colorado, Boulder, Colorado, USA
[3] University of Naples, Italy

3.0 Results

3.1 Artifical Reflectance Spectra

Figure 1 shows the results of applying the ACORN, HATCH and FLAASH atmospheric corrections to retrieve the at-sensor radiance of a 50% reflectance target modeled using MODTRAN 4 (Adler-Golden et al., 1999). The differences are most notable at the edges of the water vapor absorption bands. There are no artifacts associated with inaccurate wavelength calibration, nor sensor signal-to-noise ratio characteristics. The departures from the 50% line correspond solely with differences between the atmospheric correction models and the MODTRAN 4 model. Retrieval of the reflectance from the at-sensor radiance using MODTRAN 4 produces the straight 50% line shown in Fig. 1. The differences among models become more pronounced as the water vapor amount is increased. At 4.5 cm precipitable water vapor the FLAASH model breaks down. This problem has been corrected in later versions of the program.

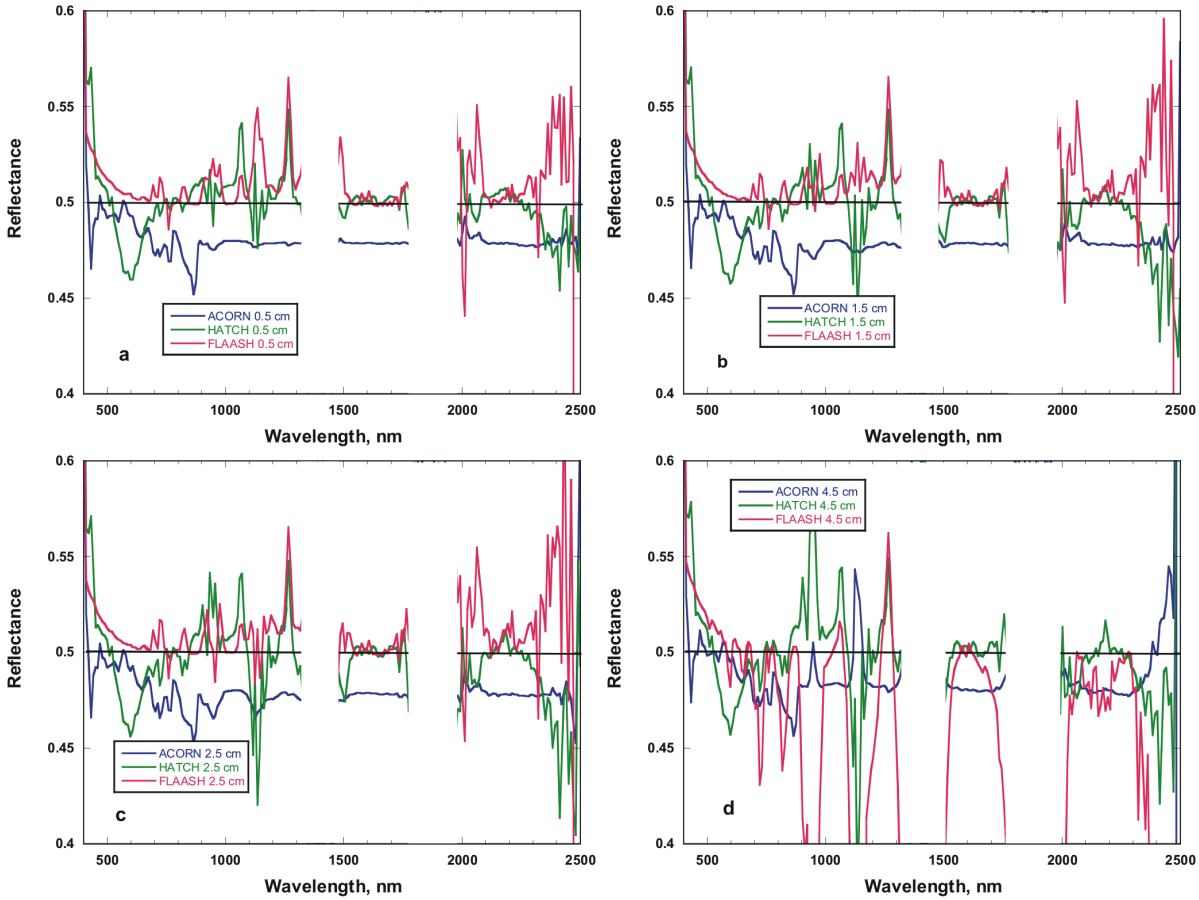

Figure 1. Model retrievals for varying total precipitable water vapor amounts. a) 0.5 cm; b) 1.5 cm; c) 2.5 cm; d) 4.5 cm. The gaps are associated with the saturated water vapor absorption features at 1380 and 1900 nm.

Sensor calibration errors lead to additional errors in the retrieval, particularly at the edges of sharp atmospheric or surface reflectance features. The errors are introduced through the process of ratioing the modeled at-sensor radiance with the measured radiance. Figure 2 shows the effects of wavelength calibration errors using a ratio of two MODTRAN 4 models convolved with the AVIRIS spectrometer point spread function and offset by 3 nm. The wavelength calibration error results in errors in reflectance of ± 20 % of the value at the edges of the sharp, unsaturated atmospheric absorption features caused by O_2, CO_2 and water vapor. Signal-to-noise ratio is important in the quality of the retrieved reflectance spectrum. Poor signal-to–noise ratio will produce artifacts at sharp absorption edges similar to those created by poor calibration shown in Fig. 2.

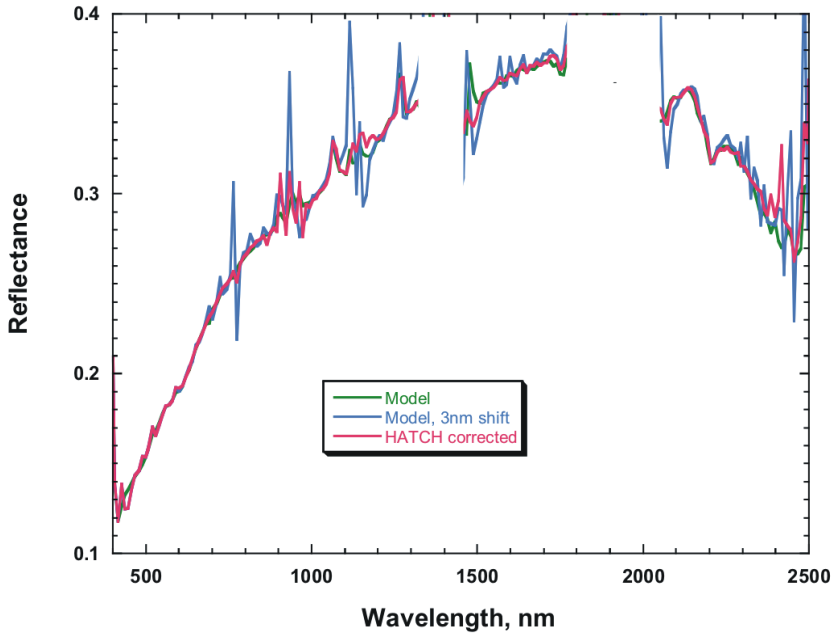

Figure 2. MODTRAN 4 model of sensor radiance from a soil surface that has been converted to reflectance using MODTRAN 4 (Model) and the same model but shifted to longer wavelengths by 3 nm. The results of the atmospheric model HATCH applied to the MODTRAN sensor radiance are shown in red.

3.2 Application to AVIRIS data

The atmospheric models were applied to AVIRIS images taken under different water vapor conditions. For comparison of the spatial quality of the water vapor effect removal, water vapor images were created. If the removal is complete, no surface albedo variability will be visible. In order to exclude the effect of sensor signal-to-noise ratio on the corrected reflectance, the entire reflectance image was averaged after the atmospheric correction was applied on a pixel-by pixel basis. Fig. 3 shows the water vapor images from the AVIRIS scene taken over Yerington, Nevada. The ATREM image (b) shows more albedo features and generally shows greater errors at high vapor values and in the presence of vegetation (Goetz et al., 2003). Fig. 4 shows the average reflectances as a result of the application of three atmospheric correction programs to correct the AVIRIS scene of Yerington, Nevada to.....???

Because the full scene is averaged, no sharp spectral reflectance features will be present. Any departure from a smooth reflectance curve is the result of an error in the model correction or an incorrect wavelength calibration. The HATCH algorithm automatically corrects for wavelength calibration errors up to ± 3 nm (Qu et al., 2003). There does not appear to be a significant wavelength calibration error because the reflectance errors at the edges of the sharp atmospheric absorption features are equivalent for each of the models.

An AVIRIS scene from Hawaii with a higher average water vapor content is shown in Figure 5.

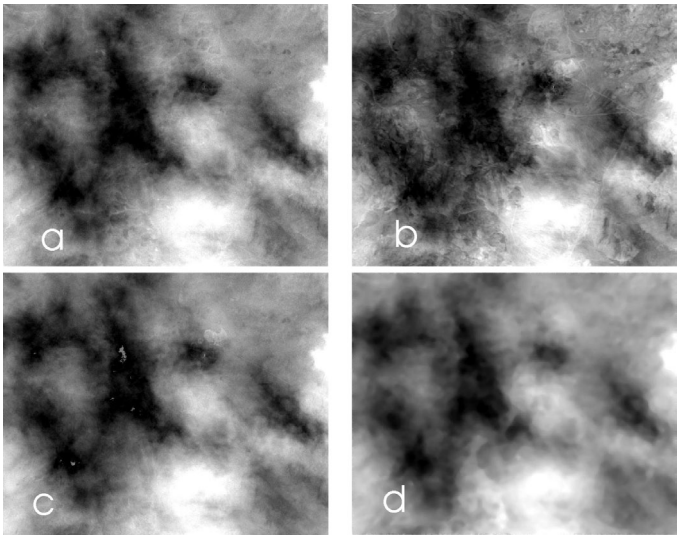

Figure 3. Water vapor images of Yerington, Nevada with average values of 0.69 cm precipitable water vapor. The models applied were a) ACORN; b) ATREM; c) FLAASH; d) HATCH

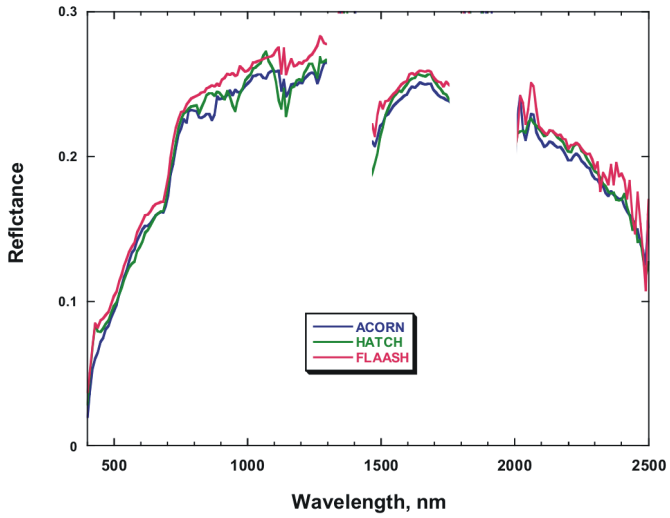

Figure 4. Reflectance derived from the Yerington scene using 3 different atmospheric correction models.

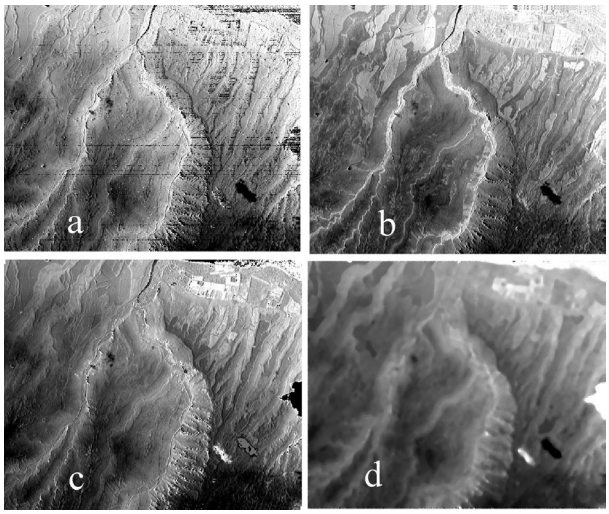

Figure 5. Water vapor images of an AVIRIS image in Hawaii. The average water vapor value is 2.21 cm. The models applied were a) ACORN; b) ATREM; c) FLAASH; d) HATCH

In this steep terrain the water vapor values are closely tied to the elevation giving the impression that the models are very sensitive to surface albedo. ATREM (b) looks the most different from the other three model images possibly reflecting higher sensitivity to vegetation cover differences. The whole-image reflectance retrievals are shown in Fig 6.

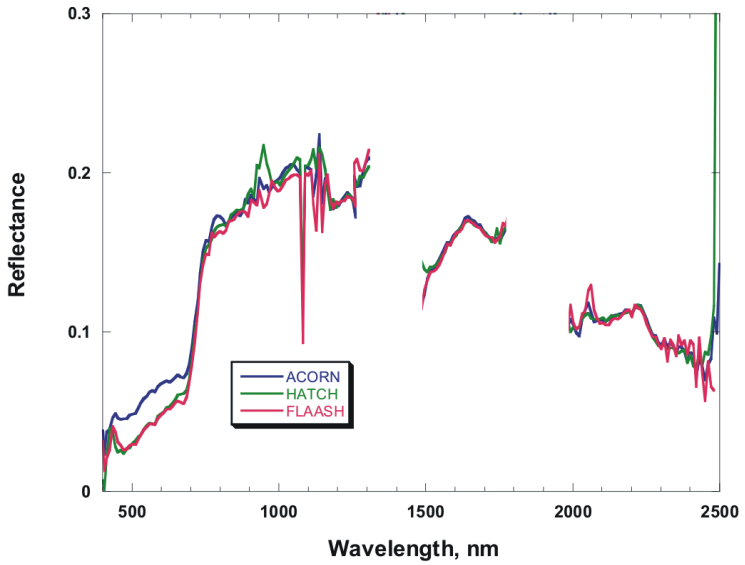

Figure 6. Reflectance averaged for the entire Hawaii scene for three correction models

The smoothest rendition of reflectance is given by ACORN but for an unknown reason the derived reflectance is considerably higher than from HATCH and FLAASH in the visible portion of the spectrum. FLAASH shows the greatest sensitivity to sharp atmospheric bands. HATCH exhibits a significant increase in reflectance around the 940 nm water vapor absorption band not shown by FLAASH or ACORN.

3.3 Application to Hyperion data

Hyperion (Pearlman et al., 2003) is a pushbroom imaging spectrometer that poses a different set of challenges for atmospheric correction. The 940 nm water vapor absorption, feature normally used to determine the column water vapor value for use in correcting the rest of the spectrum with the models, falls within the cross-over region between the two detector arrays. The signal-to-noise ratio is not high enough in this region to make an

accurate water vapor determination. As a result, the 1140 nm water vapor band is used. The difficulty here is that the calculation is more affected by the nearby deep 1200 liquid water feature in vegetation than the shallow 980 water feature near 940 nm (Goetz et al., 2003). An additional problem is the stability of the radiometric calibration and the inaccuracies in the pixel-to-pixel calibration precision leading to stripes in the images when they are enhanced by ratioing, principal components analysis or other means in which the least significant bits in the pixel values are utilized. Striping is also induced by atmospheric correction models because the small radiometric calibration errors are highlighted by ratioing the sensor radiance data with the modeled radiance. Additional artifacts are induced by sensor "smile" or the change in spectral calibration across the detector array. Smile is a characteristic of all pushbroom array systems and HATCH-2d was developed to compensate for smile by calculating the wavelength calibration for each column in the image (Qu et al., 2003). ACORN and FLAASH make use of only one wavelength calibration for each array.

Hyperion scenes having varying amounts of precipitable water vapor were processed using ACORN, HATCH-2d and FLAASH. Fig. 7 shows the water vapor images for a Hyperion scene of Yerington, Nevada. The average retrieved spectra are shown in Fig. 8.

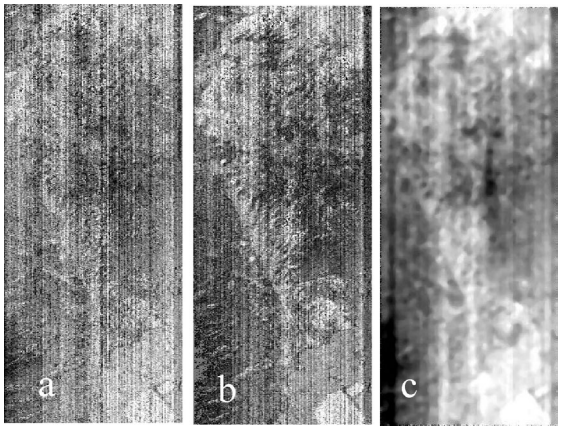

Figure 7. Water vapor images from the Hyperion scene of Yerington, Nevada. The models used were 1) ACORN; 2) FLAASH; 3) HATCH-2d. The average water vapor value is 1.26 cm.

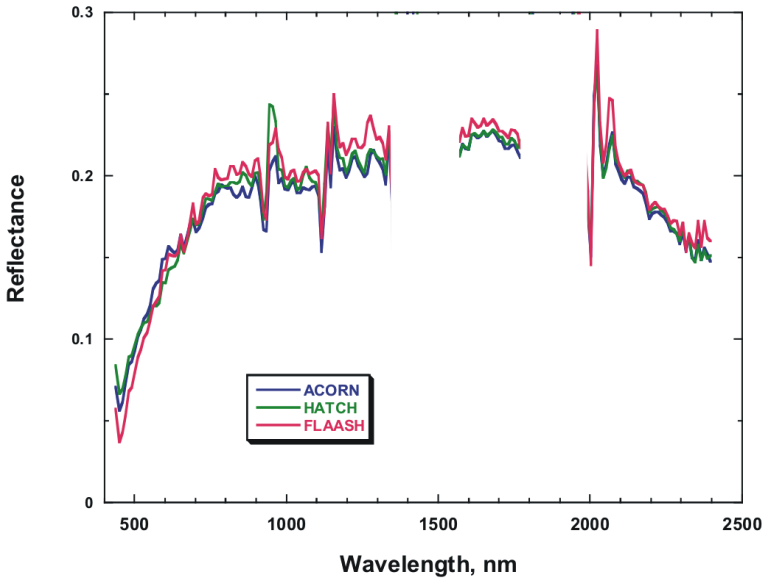

Figure 8. Reflectance spectra of the averaged Yerington, Nevada Hyperion scene.

The ragged look of the spectra is attributable to the column-to-column imprecision in radiometric calibration. In this plot the HATCH-2d column-by-column calibration was turned off. The smoothest rendition of reflectance appears to be from the ACORN model. All of the models show major departures from smooth behavior around 2050 nm, the position of two CO_2 absorption features. These features are most likely the result of wavelength calibration inaccuracies attributable to smile. In Fig. 9 the advantage of the HATCH-2d column-by-column calibration is demonstrated by switching the calibration option on. The 2050 nm CO_2 feature is significantly dampened as are some of the other water vapor band features.

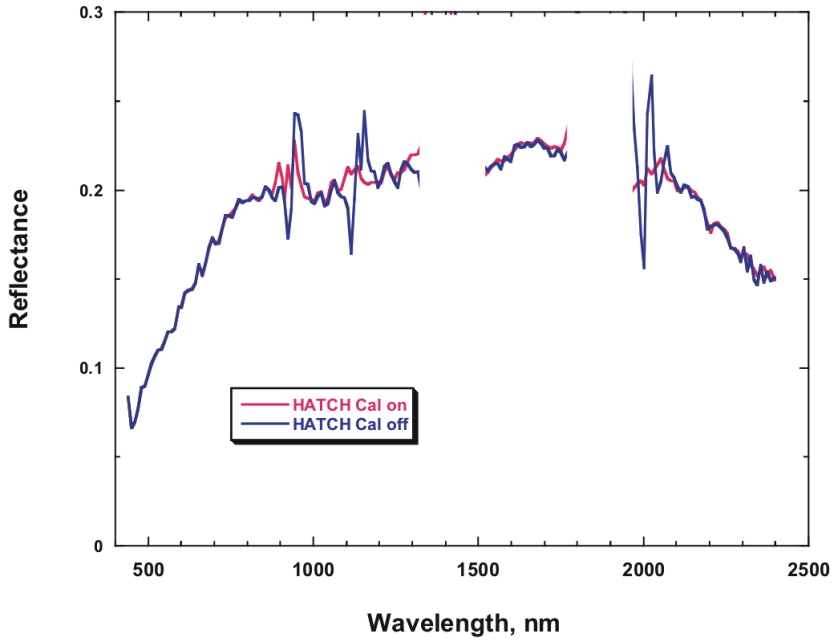

Figure 9. HATCH-2d derived reflectance of the Hyperion Yerington, Nevada scene. "HATCH Cal off" is the same curve "HATCH" shown in Fig. 8.

Figure 10 shows Table Mountain north of Boulder, Colorado. In this Hyperion scene the areas of dense vegetation were extracted and the reflectance values averaged after application of the models. Only HATCH-2d and ACORN results are shown in Fig 11.

Figure 10. CIR composite of Table Mountain, Colorado. The average water vapor value was 2.6 cm.

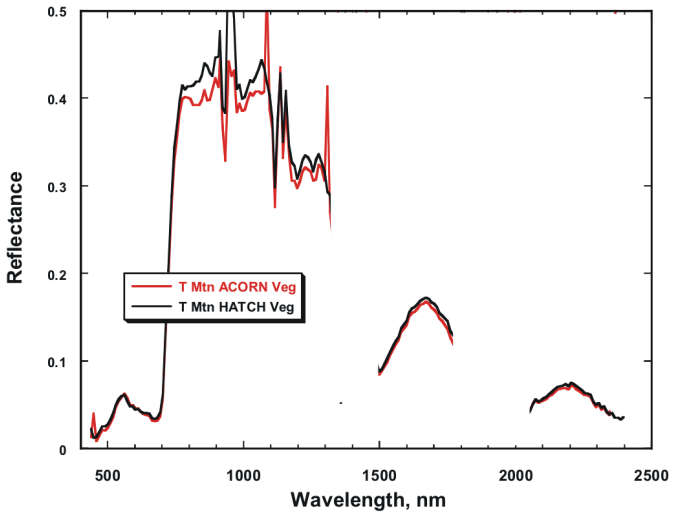

Figure 11. Average reflectances for the densely vegetated areas shown in Fig. 10.

HATCH-2d appears to provide a smoother result than ACORN in this case for the 900-1300 nm region. In the other regions the coincidence is almost perfect.

4.0 Conclusions

The results derived from artificial reflectance targets propagated through the atmosphere using MODTRAN 4 show that there are significant differences among the atmospheric correction models tested. The differences are equal to or greater than errors introduced by wavelength calibration or sensor noise. This result makes it impossible to know which model performs the best.

In retrievals from AVIRIS and Hyperion data there appears to be little to differentiate the models. In both cases the reflectances derived from scenes with higher water vapor contained more artifacts, or departures from a smooth reflectance curve.

Using HATCH-2d, with the column-by-column wavelength calibration enabled, appears to produce smoother reflectance spectra than when using an average spectral calibration for the entire array. The disadvantage is the increased computing time required.

5.0 References

Adler-Golden, S. M., M. W. Matthew, S. Bernstein, R. Y. Levine, A. Berk, S. C. Richtsmeier, P. K. Acharya, P. Anderson, J. W. Felde, J. Gardner, M. L. Hoke, L. S. Jeong, B. Pukall, A. J. Ratkowski, and H. K. Burke, H.K., 1999, Atmospheric correction for shortwave spectral imagery based on MODTRAN4, *Proceedings SPIE, Imaging Spectrometry V,* v. 3753, pp. 61–69.

Gao, B.-C., K.B. Heidebrecht, and A.F.H. Goetz, 1993, Derivation of Scaled Surface Reflectances from AVIRIS Data, *Remote Sens. Environ.*, vol. 44, 165–178.

Goetz, A.F.H., B.C. Kindel, M. Ferri, Z. Qu, 2003, HATCH: Results from simulated radiances, AVIRIS and Hyperion, *IEEE Transactions on Geoscience and Remote Sensing*, vol. 41, 1215–1222.

Matthew, M. W., S. M. Adler-Golden, A. Berk S. C. Richtsmeier, R. Y. Levin, L. S. Bernstein, P. K. Acharya, G. P. Anderson, G. W. Felde, M. P. Hoke, A. Ratkowski, H.-H. Burke, R. D. Kaiser, and D. P. Miller, 2000, Status of atmospheric correction using a MODTRAN4-based algorithm, *SPIE Proc. Algorithms for Multispectral, Hyperspectral, and Ultraspectral Imagery VI*, 4049:199–207.

Miller, C. J., 2002, Performance assessment of ACORN atmospheric correction algorithm, *Proceedings SPIE Algorithms and Technologies for Multispectral, Hyperspectral, and Ultraspectral Imagery VIII* ,v. 4725, pp. 438–449.

Pearlman, J.S., P. s. Barry, C.C. Segal, J. Shepanski, D. Beiso and S. l. Carman, 2003, Hyperion, a space-based imaging spectrometer, *IEEE Transactions on Geoscience and Remote Sensing*, vol. 41, 1160–1173.

Qu, Z., B.C. Kindel, A.F.H. Goetz, 2003, The High Accuracy Atmospheric Correction for Hyperspectral Data (HATCH) Model, *IEEE Transactions on Geoscience and Remote Sensing*, vol.41, 1223-1231.